Comparison of nanoscale measurements of strain and stress using electron back scattered diffraction and confocal Raman microscopy

Mark D. Vaudin,[1,a)] Yvonne B. Gerbig,[1] Stephan J. Stranick,[2] and Robert F. Cook[1]
[1]*Ceramics Division, National Institute of Standards and Technology, Gaithersburg, Maryland 20899, USA*
[2]*Surface and Microanalysis Science Division, National Institute of Standards and Technology, Gaithersburg, Maryland 20899, USA*

(Received 26 September 2008; accepted 24 October 2008; published online 13 November 2008)

Stresses in Si as small as 10 MPa have been measured using electron backscattered diffraction (EBSD) and confocal Raman microscopy (CRM) with spatial resolutions of 10 nm and 100 nm, respectively. In both techniques, data were collected across wedge indentations in (001) Si. EBSD measured the stress and strain tensors and CRM measured the uniaxial stress. The results agreed very well except close to the indentation, where the surface-sensitive EBSD results indicated larger stresses. Results converged when the CRM laser excitation wavelength was reduced, probing smaller depths. The stress profiles are consistent with the inverse-square power law predicted by Eshelby analysis. © *2008 American Institute of Physics*. [DOI: 10.1063/1.3026542]

The ability to measure stress or strain at the nanoscale is a significant factor in decreasing the development time and increasing the manufacturing yield and operational reliability of advanced devices in a number of technology areas. Stress-engineered channels with increased carrier mobility have been in use since the 90 nm semiconductor technology node and are expected to play a large role in improving microelectronic device performance as dimensions shrink even further.[1] Substrate effects on photonic quantum-well structures lead to differences in strain states and thus changes in the output color and lifetime of visible light-emitting and laser diodes.[2] Stress concentrations in components of microelectromechanical systems (MEMS) lead to fracture and buckling that truncate the reliability of MEMS devices.[3] Clearly, a method to measure stress or strain at the nanoscale would enable device developers to optimize materials and processing selections more readily for optimum device performance. Two techniques that show great promise for such measurements and have adequate resolution, both spatially and in terms of stress and strain, are electron back scattered diffraction (EBSD) and confocal Raman microscopy (CRM). Both EBSD and CRM are well suited to the study of stresses in silicon. This letter describes a detailed study comparing the results of these two techniques applied to the same silicon samples.

In the EBSD method, cross correlation is applied between selected regions of interest (ROIs) in high-quality EBSD patterns obtained from the sample surface using an EBSD detector installed in a scanning electron microscope (SEM). A pattern obtained from a strain-free part of the sample is chosen as the reference pattern and the other patterns are cross-correlated against that reference. The technique determines the complete strain tensor and also the rigid body rotations;[4] the stress tensor is determined from the strain tensor and the material elastic constants. (Note, however, that the measurement is insensitive to hydrostatic strain.) The analysis has been implemented in commercial software.[5] In the CRM method, a Raman spectrum is obtained at each pixel of an analyzed area and the position of the Si Raman peak at $\approx 521\ \mathrm{cm}^{-1}$ is determined. The position of this peak is compared to that in a reference spectrum obtained from strain-free material (in an analogous fashion to the EBSD technique) and the difference is converted to a stress by multiplication by a constant related to the Si phonon deformation potentials (PDPs).[3,6,7] (Nonhydrostatic stress breaks the degeneracy of the three Raman phonon modes leading to an apparent peak shift.) Note that both techniques measure changes relative to an assumed strain-free region and do not measure absolute unit cell dimensions.

The test samples in this study were 3 mm thick parallel-sided (001) orientation Si disks 35 mm in diameter[8] that had been indented with a diamond linear wedge indenter to a peak load of 350 mN. The long axis (or tip) of the diamond wedge was 20 μm long and the wedge angle was 140°. The wedge axis was aligned along [110] during indentation. In the center of the indentation the strain field associated with the residual contact impression was unvarying parallel to the impression so that perpendicular line scans across the impression performed by EBSD and CRM could be compared readily. A Cartesian coordinate system was used with the z-axis normal to the surface along [001], the y-axis in the plane of the sample surface parallel to the long axis of the contact impression along [110], and the x-axis in the plane of the sample surface perpendicular to the impression axis along $[1\bar{1}0]$.

The EBSD data collection was carried out in a Hitachi 4700 field emission SEM equipped with a Nordlys detector (HKL-Oxford Instruments).[9] The microscope was operated at 30 kV with an excitation current of 30 μA, and the probe current measured by Faraday cup during the experiments was about 3 nA. The probe diameter was of the order of 2 nm and the sample was tilted to 70°. Line scans across the center of the indentation in the x direction were carried out with a 200 nm step size; the scans typically consisted of 400 points. The integration time for the diffraction pattern at each pixel was about 2 s and the patterns were all stored for subsequent analysis. The line scans were short enough in duration that drift was insignificant, as confirmed by images recorded before and after the scans. Each pattern was stored as uncompressed, 8-bit gray scale in jpeg format, 1344×1024 pixels and analyzed using the CROSSCOURT software package.[5] The patterns were cropped to 1024×1024 pixels

a)Electronic mail: mark.vaudin@nist.gov.

 © 2008 American Institute of Physics

Author complimentary copy. Redistribution subject to AIP license or copyright, see http://apl.aip.org/apl/copyright.jsp

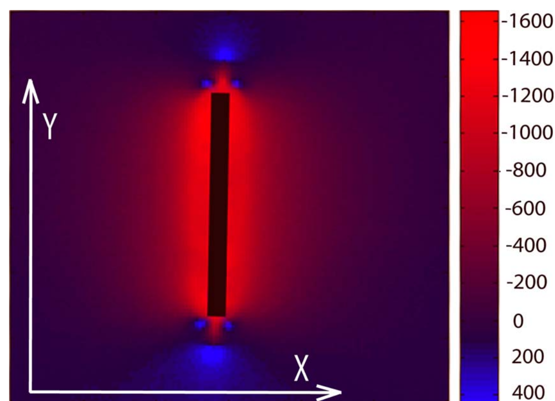

FIG. 1. (Color online) CRM stress map of 350 mN wedge indentation in Si obtained using 488 nm excitation wavelength. Stresses are in megapascals.

by removing equal sized areas from both sides. ROIs 256 $\times 256$ pixels were distributed over the pattern with one at the center and the rest distributed evenly around the edge; typically, 20 ROIs were used. High and low pass filter levels were set to reduce the effects of image noise and variation in image intensity, respectively. The analysis procedure for each pattern was to cross correlate each ROI in the pattern with its counterpart in the reference pattern, thus determining the change in the vector joining the electron impact point to the center of the ROI. From these pattern distortion measurements, the strain and stress tensors at each sample point were determined.[4]

The CRM data were collected using a custom system based on a system described elsewhere.[10] Briefly, laser radiation passed through a polarizer and an "inject-reject" notch filter, and was focused on the sample using a 60$\times$ oil-immersion lens of numerical aperture 1.4. Scattered Raman light was collected by the lens, passed back through the notch filter, and collected with a spectrograph. Single-mode optical fibers coupled the laser and spectrograph to the system to provide an input Gaussian beam and confocal imaging of the output scattered light. An *x*-*y* stage with closed-loop control with 10 nm resolution allowed for scanning of the laser; with oversampling, the spatial resolution of the technique was close to 100 nm, depending on the wavelength of the laser excitation. Three laser wavelengths were used 633 nm, 532 nm, and 488 nm. The penetration of the laser light varies strongly with wavelength and the information depths for the wavelengths were 1.3 μm, 400 nm, and 250 nm, respectively.[11] The incident excitation was polarized along [110] (*y*) with a rejection ratio of 10^5; thus, the technique is principally measuring σ_{xx} and is almost completely insensitive to σ_{yy}. As in the case of the EBSD experiment, *x*-direction line scans across the wedge indentations were collected, with a step size of 120 nm. In addition, stress maps were obtained using full *x*-*y* scans. A Raman spectrum was obtained at each analysis point and the position of the Raman peak determined by fitting a Pearson VII function to the data, from which the shift of the peak was found. In the geometry used for these experiments, the Raman shift is determined by the stress in the plane of the wafer. As the stress state near the surface adjacent to the linear contact impression was expected (and shown) to be nearly uniaxial σ_{xx}, the constant of proportionality linking the stress to the shift in the peak position was taken as -435 MPa/cm^{-1}.[3]

Figure 1 shows a Raman stress map of a 350 mN wedge-

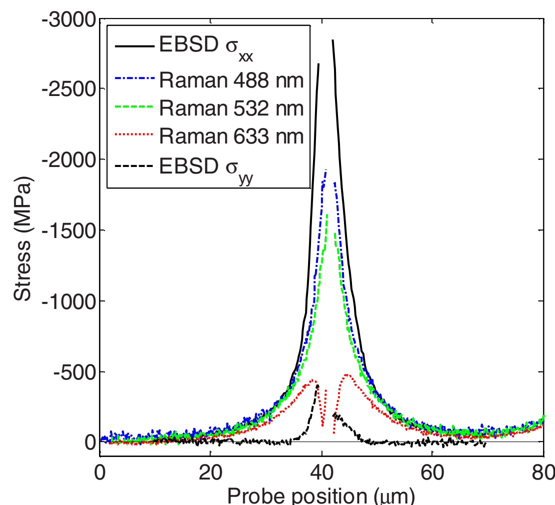

FIG. 2. (Color online) Stress profiles across a 350 mN wedge indentation in Si measured using CRM at three laser wavelengths and EBSD.

indentation impression obtained using 488 nm excitation. As with other such Raman-based stress maps of indented[12,13] or scratched[14] Si, the stress field is complicated and heterogeneous, with both tensile and compressive regions (weak scattering at 521 cm^{-1} in the center of the impression in the plastic deformation zone[8] does not allow the stress level to be determined at those points). The stress-field heterogeneity is not considered in detail here, but it is noted that the compressive stress is great and nearly invariant with *y* in the central region adjacent to the indentation and decreases significantly away from the indentation in the *x* direction on either side.

Figure 2 shows the stress field across a similar indentation measured with both EBSD and CRM. For the EBSD measurements, σ_{xx} and σ_{yy} are plotted, and for the CRM, the σ_{xx} stress measured from the Raman shift using the three wavelengths listed above is plotted. At this indentation load (350 mN), the wedge indenter penetrated the Si surface to a peak depth of 530 nm and left a residual impression 160 nm deep. EBSD data show that the stress parallel to the indentation σ_{yy} is zero except close to the indentation where it rises to about an order of magnitude smaller than σ_{xx}, the stress normal to the indentation. Thus the stress state is primarily uniaxial, and direct comparison can be made between σ_{xx} determined by EBSD and the stress determined by simple scalar multiplication of the Raman shift.[3,7] The agreement between these two measurements improved as the Raman excitation laser wavelength was decreased and further than 6 μm from the indentation, the 488 nm CRM and EBSD data agree perfectly (within the noise); nearer the indentation, the EBSD stresses are larger. The interpretation of these observations is that the information depths of the CRM technique given above for the various laser wavelengths are all at least an order of magnitude larger than the EBSD information depth. Si recovers significantly on indentation unloading and the residual stress field associated with the remnant contact impression is concentrated adjacent to the impression, decreasing significantly with increasing *x* (Figs. 1 and 2), but also with increasing *z* into the material.[8]

The indentation studied was at the end of a row of indentations 50 μm apart, and on the right side of Fig. 2 the stress increases, with a minimum 25 μm from the center of the indentation stress field (i.e., half way to the next inden-

Author complimentary copy. Redistribution subject to AIP license or copyright, see http://apl.aip.org/apl/copyright.jsp

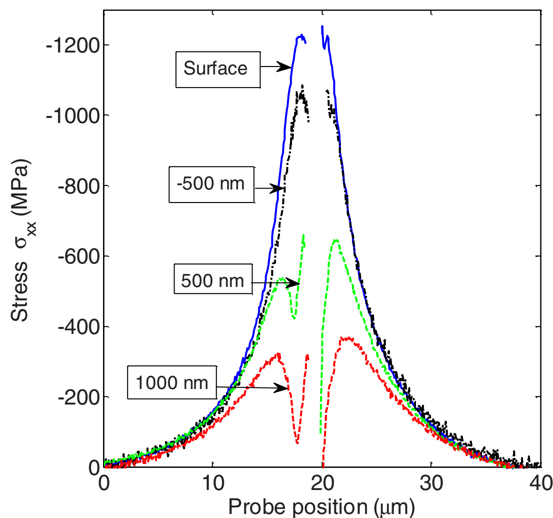

FIG. 3. (Color online) Stress profiles across a 350 mN wedge indentation in Si collected at different focal depths.

tation), but on the left the stress decays toward zero. Similar data were collected from three other indentations in the row and it was clear that both techniques had sufficient stress resolution to detect the overlapping stress fields of adjacent indentations. The simplicity of the uniaxial surface stress field of the wedge-indentation test structure permitted direct comparison of the stresses inferred from the EBSD and CRM measurements, something not possible with the more complicated test structures used in a previous diffraction comparison using transmission electron microscopy.[15] Previous studies of uniaxially (bent beam)[3] and biaxially (flexed wafer)[16] stressed Si systems, in which the stress in the sample was determined from displacement measurements or calculated from analytical or finite element models, show very good agreement with the stresses determined from CRM measurements using the same PDPs (Ref. 6) used here. The agreement between the CRM and EBSD measurements at similar information depths provides further support that the PDPs of Anastassakis *et al.*[6] are the best choice for CRM determination of stress in Si.

The CRM data presented in Fig. 2 were collected with the laser light focused at the sample surface. Other data were collected with the focus 0.5 μm above the surface and 0.5 and 1.0 μm below the surface. Figure 3 shows CRM data collected in x-direction scans across an indentation at these four focal planes. The greatest stresses were measured with the focus at the surface, and focusing either above or below the surface decreased the observed stresses substantially. In addition, the sharp dips in the data observed in the +0.5 and +1.0 μm curves at about 18 μm are indicative of subsurface cracking, resulting in stress relief, which is not apparent at and above the surface. These through-focus data indicate that the stress varies in both the x and z directions. The residual indentation stress field in the x-z plane can be modeled as that arising from an expanding cylinder[17,18] in an infinite medium; such a stress field falls off radially as the inverse square of the distance from the cylinder axis. The variation in the EBSD-measured stress σ_{xx}, as a function of distance x, from the indentation center (in the decreasing x direction of Fig. 2, i.e., away from any neighboring indentations) was fitted with a power-law function $\sigma(x)=a(x+b)^c+d$. The fit yielded $c=-1.89\pm0.17$, where the uncertainty represents 95% confidence bounds. A fit of the same function to the 488 nm CRM data gave $c=-1.92\pm0.22$. In both cases, the exponent is very close to the ideal value of -2, and the fits are consistent with the idea that the localized plastic deformation zone generated by the wedge contact acts as an expanding cylinder imbedded in the surrounding elastic matrix similar to damage generated by sharp, rolling contacts.[18]

Both the EBSD and CRM techniques are powerful methods for measuring stress at the nanoscale, each with its particular strengths. The spatial resolution of EBSD is about an order of magnitude better than CRM, although CRM has the ability to probe below the sample surface using both changes in excitation wavelength and focal plane. EBSD can be used to determine the strain tensor and rigid body rotations directly from the diffraction patterns, and using the material elastic constants, the complete stress tensor can then be determined. The opportunity thus exists for implementing off-axis, polarized excitation and analysis CRM,[16,19] which can determine the components of the stress tensor for direct comparison with EBSD. The stress resolution approaches 10 MPa in Si for both techniques and the speed of the two methods is similar; data can be collected at the rate of about one measurement per second. The CRM technique can be carried out in ambient and EBSD requires a vacuum environment. The success in measuring strains and stresses at the resolutions reported here show that one of the holy grails of nanocharacterization[1–3] is being attained.

[1] A. M. Noori, M. Balseanu, P. Boelen, A. Cockburn, S. Demuynck, S. Felch, S. Gandikota, A. J. Gelatos, A. Khandelwal, J. A. Kittl, A. Lauwers, W.-C. Lee, J. Lee, T. Mandrekar, R. Schreutelkamp, K. Shah, S. E. Thompson, P. Verheyen, C.-Y. Wang, L.-Q. Xia, and R. Arghavani, IEEE Trans. Electron Devices **55**, 1259 (2008); R. Arghavani and H. M'Saad, Solid State Technol. **51**, 327682 (2008).

[2] J. S. Hwang, A. Gokarna, Y.-H. Cho, J. K. Son, S. N. Lee, T. Sakong, H. S. Paek, O. H. Nam, Y. Park, and S. H. Park, J. Appl. Phys. **102**, 013508 (2007).

[3] V.T. Srikar, A.K. Swan, M. Selim Ünlü, B. B. Goldberg, and S.M. Spearing, J. Microelectromech. Syst. **12**, 779 (2003).

[4] A. F. Wilkinson, G. Meaden, and D. J. Dingley, Ultramicroscopy **106**, 307 (2006).

[5] A. F. Wilkinson, G. Meaden, and D. J. Dingley, Mat. Sci. Technol. **22**, 1271 (2006).

[6] E. Anastassakis, A. Cantareo, and M. Cardona, Phys. Rev. B **41**, 7529 (1990).

[7] I. De Wolf, Semicond. Sci. Technol. **11**, 139 (1996).

[8] R. F. Cook, J. Mater. Sci. **41**, 841 (2006).

[9] Any mention of commercial products in this paper is for information only; it does not imply recommendation or endorsement by NIST.

[10] C. E. Jordan, S. J. Stranick, R. R. Cavanagh, L. J. Richter, and D. B. Chase, Surf. Sci. **433**, 48 (1999).

[11] M. J. Pelletier, *Analytical Applications of Raman Spectroscopy* (Blackwell Scientific, Oxford, 1999).

[12] M. Bowden and D. J. Gardiner, Appl. Spectrosc. **51**, 1405 (1997).

[13] U. Schmidt, W. Ibach, J. Müller, K. Weishapt, and O. Hollricher, Vib. Spectrosc. **42**, 93 (2006).

[14] E. Bonera, M. Fanciulli, and D. Batchelder, J. Appl. Phys. **94**, 2729 (2003).

[15] V. Senez, A. Armigliato, I. De Wolf, G. Carnevale, R. Balboni, S. Frabboni, and A. Benedetti, J. Appl. Phys. **94**, 5574 (2003).

[16] G. H. Loechelt, N. G. Cave, and J. Menéndez, J. Appl. Phys. **86**, 6164 (1999).

[17] R. Hill, *The Mathematical Theory of Plasticity* (Oxford University Press, Oxford, 1986).

[18] B. L. Symonds, R. F. Cook, and B. R. Lawn, J. Mater. Sci. **18**, 1306 (1983).

[19] R. Ossikovski, Q. Nguyen, G. Piccardi, and J. Schreiber, J. Appl. Phys. **103**, 093525 (2008).

Author complimentary copy. Redistribution subject to AIP license or copyright, see http://apl.aip.org/apl/copyright.jsp